Optical Materials: X 15 (2022) 100169

Contents lists available at ScienceDirect

Optical Materials: X

journal homepage: www.journals.elsevier.com/optical-materials-x

Luminescence properties and time-resolved spectroscopy of rare-earth doped $SrMoO_4$ single crystals

Viktorija Pankratova [a,*], Elizaveta E. Dunaeva [b], Irina S. Voronina [b], Anna P. Kozlova [c], Roman Shendrik [d], Vladimir Pankratov [a]

[a] Institute of Solid State Physics, University of Latvia, 8 Kengaraga iela, LV-1063, Riga, Latvia
[b] Prokhorov General Physics Institute, Russian Academy of Sciences, Vavilov Str. 38, Moscow, Russia
[c] National University of Science and Technology «MISiS», Leninsky Pr. 4, 119049, Moscow, Russia
[d] Vinogradov Institute of Geochemistry, SB RAS, 1a Favorskii Street, 664033, Irkutsk, Russia

ARTICLE INFO

Keywords:
$SrMoO_4$
Eu^{3+}
Pr^{3+}
Photoluminescence
Time-resolved spectroscopy

ABSTRACT

Luminescence properties of nominally pure and doped with Eu^{3+} and Pr^{3+} ions $SrMoO_4$ single crystals grown by the Czochralski method have been studied. Thermal quenching of intrinsic emission of pure and doped $SrMoO_4$ single crystals has been observed, as well as a correlation of thermal quenching activation energies with rare-earth ion concentration has been observed. Tunable laser was used to study time-resolved luminescence in a range from 10 K to room temperature. The effect of dopant nature and concentration on intrinsic emission and decay kinetics has been elucidated.

1. Introduction

Molybdates $MMoO_4$ (M = Ca, Sr, Pb, Cd) are scheelite-type compounds that have attracted interest in the light of various features, mainly pertaining to photocatalysis and pigments, but also including fluorescent and scintillating materials [1–4]. In particular, $CaMoO_4$ is known for its fluorescence ranging from blue to green emission, depending on specific doping and crystallinity [5]. Optical and luminescence properties of rare-earth (RE) doped $SrMoO_4$ single crystals so far have been studied poorly compared with other molybdates.

$SrMoO_4$ is a material with a 4.7 eV band gap [6] which exhibits intrinsic luminescence due to transition from a filled 2p orbital of O^{2-} to an empty 4d orbital of Mo^{6+} [7]. Trivalent rare-earth ions (RE^{3+}) substitute Sr^{2+} because of similar radii which, however, causes the need to compensate the mismatch of charges, for example, by using alkali metal ions [8] for local charge compensation or pentavalent ions to substitute Mo^{6+} in the oxygen tetrahedra [9].

2. Experimental

2.1. Samples

$SrMoO_4$ single crystals studied in current research (Fig. 1) have been grown utilizing the Czochralski method with a weight and growth control program at Prokhorov General Physics Institute of the Russian Academy of Sciences (Moscow, Russia). The details of the crystals' growth have been reported in Ref. [9]. Pure and doped with $PrNbO_4$ (1.0 wt%) and different concentrations of $EuNbO_4$ (0.1 wt%, 0.22 wt% and 0.5 wt%) single crystals have been studied. Doping with Pr^{3+} and Eu^{3+} in form of niobate salts was implemented in order to achieve local charge compensation as was described in Ref. [9].

2.2. Optical and luminescence measurements

Optical absorption spectra of the crystals have been measured at room temperature with a Perkin Elmer Lambda 950 spectrophotometer.

Electron paramagnetic resonance (EPR) spectra have been recorded utilizing a RE-1306 X-band spectrometer (Russia) with a frequency of 9.358 GHz. Magnetic field was oriented along c axis of the samples. Double integrals of the EPR signal of each sample doped with different Eu concentrations were calculated to obtain Fig. 3.

Luminescence excitation and emission spectra at room temperature have been obtained using photoluminescence spectrometer FLS1000 (Edinburgh instruments). Time-resolved luminescence spectra, as well as luminescence emission spectra under room temperature, have been studied upon excitation by wavelength-tunable pulsed solid-state laser

* Corresponding author. Nano and Molecular Systems Research Unit, University of Oulu, FIN-90014, Finland.
E-mail address: viktorija.pankratova@cfi.lu.lv (V. Pankratova).

https://doi.org/10.1016/j.omx.2022.100169
Received 31 December 2021; Received in revised form 26 June 2022; Accepted 4 July 2022
Available online 22 July 2022

Ekspla NT342/3UV (210–2300 nm). The emission signal was detected by the Andor iSTAR DH734-18 mm CCD camera coupled to the Andor SR-303i-B spectrometer. Luminescence decay kinetics were measured by a photomultiplier tube PG122 (time resolution better than 5 ns) and digital oscilloscope Tektronix TDS 684A.

3. Results and discussion

3.1. Absorption

A visible change of colour has been observed in the single crystals of $SrMoO_4$ with increasing concentration of $EuNbO_4$ where the most intensive shade of brown belongs to the $SrMoO_4$:0.5% $EuNbO_4$. Change in colours is based on a broad absorption band in the region of 3 eV (Fig. 2) which is absent in the case of nominally pure $SrMoO_4$ single crystal. With an increase of $EuNbO_4$ concentration the intensity of this absorption band increases, as well as the position of its maximum changes towards the lesser energies. The absorption of divalent Eu ions has been observed in the $SrMoO_4$ matrix for the first time. However, a similar wide band peaked at 2.5 eV has been previously observed in $CaMoO_4$ single crystal, annealed in the reducing atmosphere [10].

This broad absorption band around 3 eV corresponds to 4f-5d transitions of Eu^{2+} ions which replace Sr^{2+} ions in the $SrMoO_4$ matrix. Correspondence to Eu^{2+} 4f-5d transitions has been made because the intensity of the characteristic EPR signals of Eu^{2+} [11] is dependent on the absorption band area and the concentration of $EuNbO_4$ accordingly (Fig. 3). Due to 5d energy level of Eu^{2+} being in the conduction band of the crystal, the 4f-5d transition is optically inactive and does not produce luminescence by exciting the crystals at 3 eV.

The absorption spectrum of Pr doped single crystal is shown in the supplementary materials (Fig. S1).

3.2. Luminescence properties

The luminescence properties of rare-earth doped $SrMoO_4$ single crystals are based on the luminescence of the molybdate complex, as well as trivalent rare-earth ions. The luminescence emission spectra of pure $SrMoO_4$ crystal at room temperature are shown in Fig. 4. The luminescence excitation spectra of pure $SrMoO_4$ crystal at room temperature with emission at 520 nm are shown in Fig. 5. Luminescence excitation spectra of non-activated $SrMoO_4$ crystal are characterized by a broad MoO_4^{2-} ligand-to-metal charge transfer (LMCT) band with maximum intensity at 275–300 nm which has the same excitation

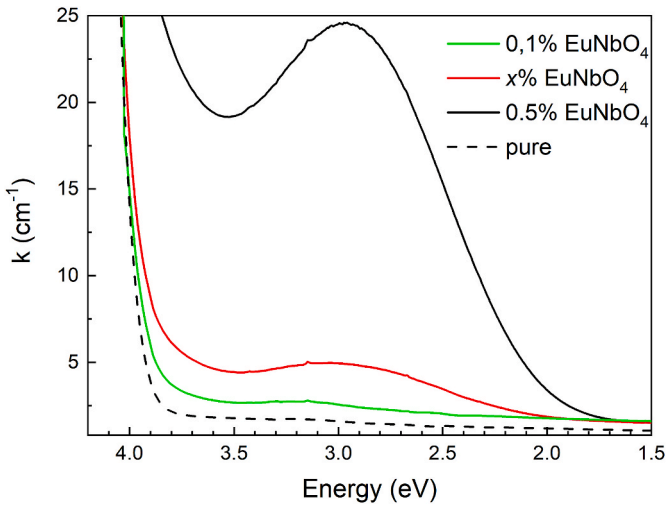

Fig. 2. Absorption spectra of nominally pure and with Eu doped $SrMoO_4$ single crystals at room temperature.

mechanism as other molybdates [5–7], as well as tungstates and vanadates [7,12,13]. On the other hand, under excitation an electron transfers from O^{2-} to Mo^{6+}, which creates electron-hole pairs on Mo and O sites respectively within one anion complex. This may also be considered as a Frenkel exciton and LMCT band – as an excitonic band accordingly. A less intensive broad excitation band is also present with a maximum intensity at 360–370 nm. A possible explanation of a less intensive broad with a red shift from the excitonic band is that it is caused by a defect of a crystal which is acting as an electron trap in a band gap of the $SrMoO_4$ single crystal. Based on the knowledge of other complex oxides we assume that such defect can be F-type centers. Therefore, it can be concluded that the luminescence emission spectrum in Fig. 5 is formed due to the excitation of both the excitonic band and the defect of the $SrMoO_4$ crystal.

The luminescence emission spectra of $SrMoO_4$ crystals doped with different concentrations of Eu^{3+} are shown in Fig. 6 and the luminescence emission spectra of $SrMoO_4$ doped with Pr^{3+} ions – in Fig. 8. By exciting the single crystals studied in the LMCT broad band Eu^{3+} and Pr^{3+} sharp 4f-4f lines are seen in the luminescence spectra which indicates energy transfer to energy levels of rare-earth ions in the band gap. Energy and terms of Eu^{3+} and Pr^{3+} 4f-4f lines correspond to the

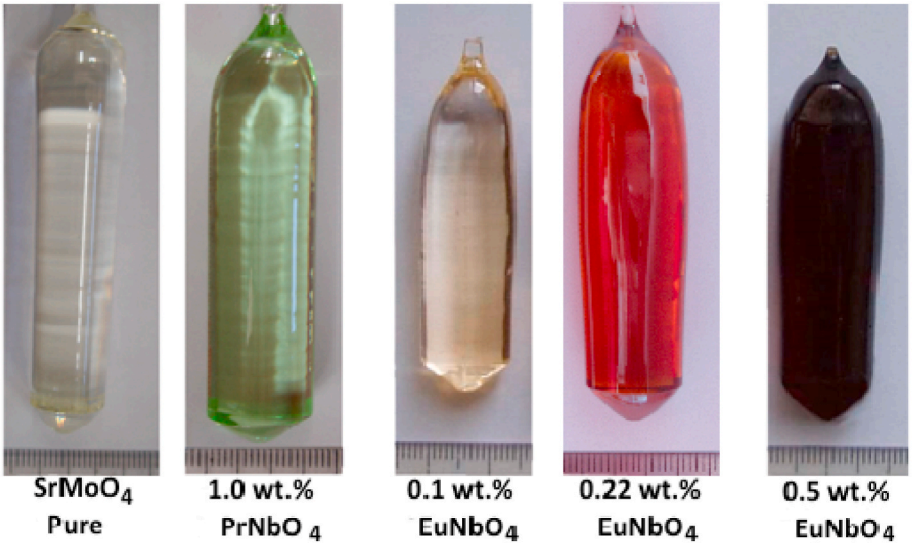

Fig. 1. Pure and doped $SrMoO_4$ as-grown crystals.

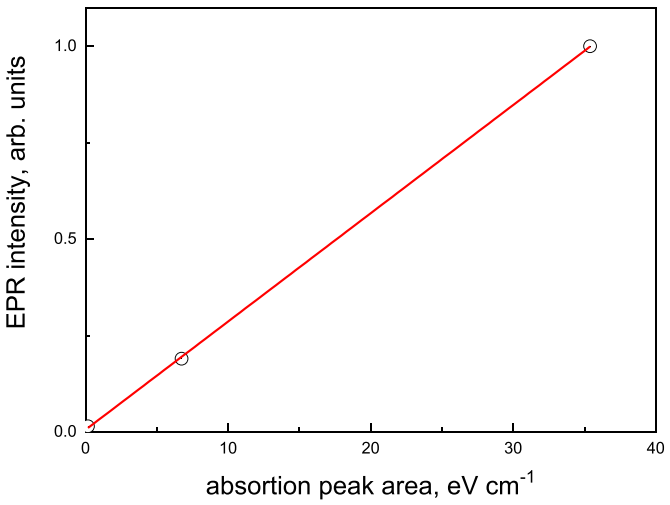

Fig. 3. Dependency of Eu^{2+} EPR integral intensity from the area of the absorption band in the region of 3 eV. The intensity of the EPR signal denoted as 1 has been taken as the relative intensity of an EPR signal in $SrMoO_4$:Eu (0.5 wt % $EuNbO_4$).

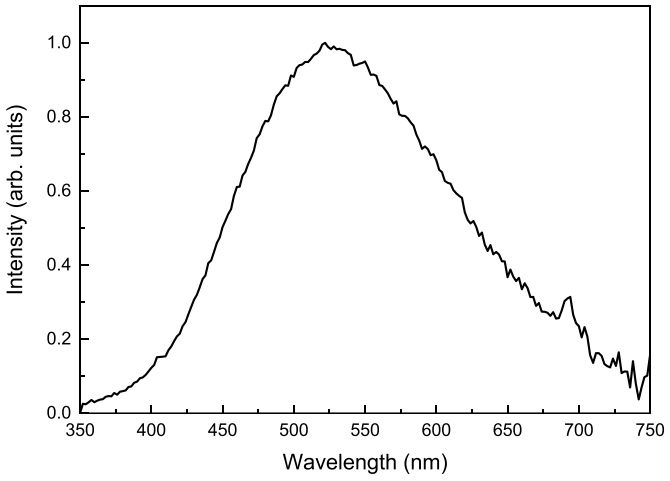

Fig. 4. Luminescence spectrum of pure $SrMoO_4$ crystal at room temperature normalized at maximum luminescence intensity (luminescence excitation at 300 nm).

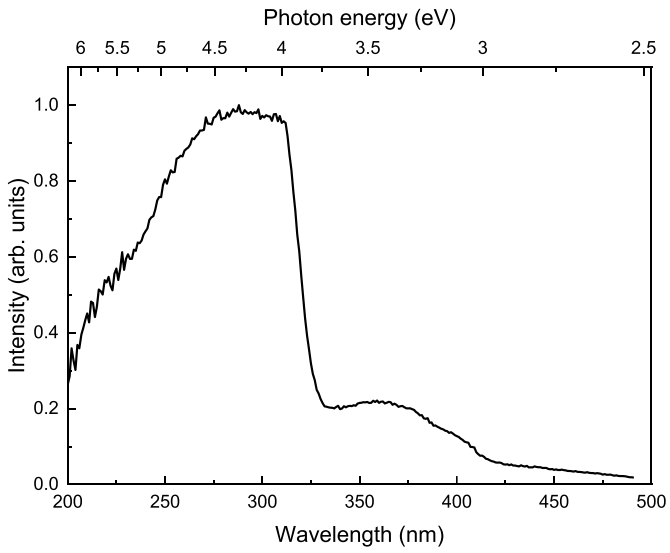

Fig. 5. Luminescence excitation of pure $SrMoO_4$ crystal at room temperature normalized at maximum excitation intensity (luminescence emission at 520 nm).

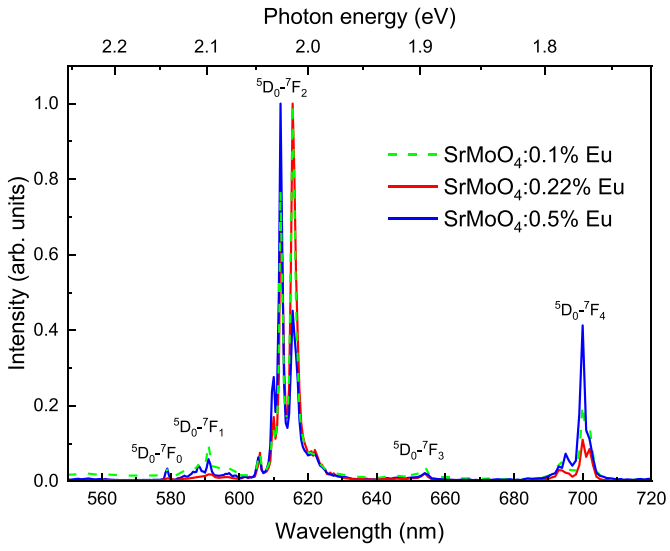

Fig. 6. Luminescence emission spectra at room temperature of $SrMoO_4$ crystals doped with different concentrations of Eu^{3+} (luminescence excitation 300 nm). Luminescence spectra are normalized at maximum intensity.

literature [3,6,14–16]. The emission lines of Eu^{3+} correspond to $^5D_0$-^7F_J transitions, the most intensive ones being the transitions to energy levels with terms $^5F_2$ and $^5F_4$. Fig. 6 shows that in the case of $SrMoO_4$ single crystal with the lowest Eu^{3+} concentration a very broad band with low intensity (550–580 nm) exists. This broad band corresponds to non-intensive LMCT emission signifying the uncomplete energy transfer from LMCT to Eu^{3+} energy levels. LMCT emission band has a very low intensity at room temperature.

As one sees from Fig. 6 also the ratio of intensities of the $^5D_0$-$^7F_2$ lines changes which is dependent on the Stark splitting of the $^7F_2$ energy levels of Eu^{3+} ion under influence of the change of the crystal's symmetry by increasing $EuNbO_4$ concentration [6,17,18].

Luminescence excitation spectra of Eu-doped $SrMoO_4$ single crystals (Fig. 7) consist of several sharp 4f-4f transitions of Eu^{3+} ions from the $^7F_0$ term. These 4f-4f transitions of Eu^{3+} ions coincide with the literature data and are characteristic of Eu^{3+} ions [6,15,19]. The intensity of Eu^{3+} 4f-4f signals decreases greatly with the increase of $EuNbO_4$ concentration due to concentration quenching of Eu^{3+} ions.

A broad band in the UV region of the excitation spectra (Fig. 7) represents the charge transfer process from O^{2-} to Mo^{6+}. However, an increase in $EuNbO_4$ concentration shifts the position of the LMCT band towards the higher energies. This blue shift of the band happens when the competitive process of the charge transfer from O^{2-} to Eu^{3+} occurs [6,20,21]. The shift can also be assigned to another possible competitive charge transfer from O^{2-} to Nb^{5+} [19]. The LMCT band also deforms visibly because of several charge transfer processes competing with each other.

The luminescence emission spectra (Fig. 8) of Pr-doped $SrMoO_4$ show intensive Pr^{3+} 4f-4f signals. By exciting the $SrMoO_4$:Pr^{3+} single crystal in the LMCT band, a broad emission band of low intensity can be observed in the region from 400 nm to 720 nm. This emission band corresponds to the one observed in nominally pure $SrMoO_4$ single crystal (Fig. 4). The nature of the broad LMCT emission band with low intensity is proven by the lack of it while exciting Pr^{3+} ions directly (transition $^3H_4$–$^3P_2$). The luminescence excitation spectra of $SrMoO_4$:Pr single crystal (Fig. 9) consists of LMCT excitation band and Pr^{3+} 4f-4f lines, similarly as in the case of Eu-doped $SrMoO_4$ single crystals. The

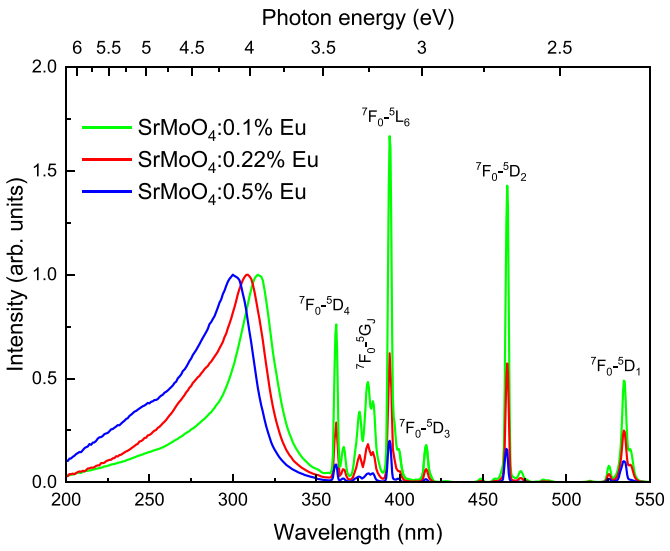

Fig. 7. Luminescence excitation spectra at room temperature of $SrMoO_4$ single crystals doped with different concentrations of $EuNbO_4$ (luminescence emission 616 nm which corresponds to Eu^{3+} transition $^5D_0$-$^7F_2$). Luminescence spectra are normalized at the maximum intensity of LMCT excitation band.

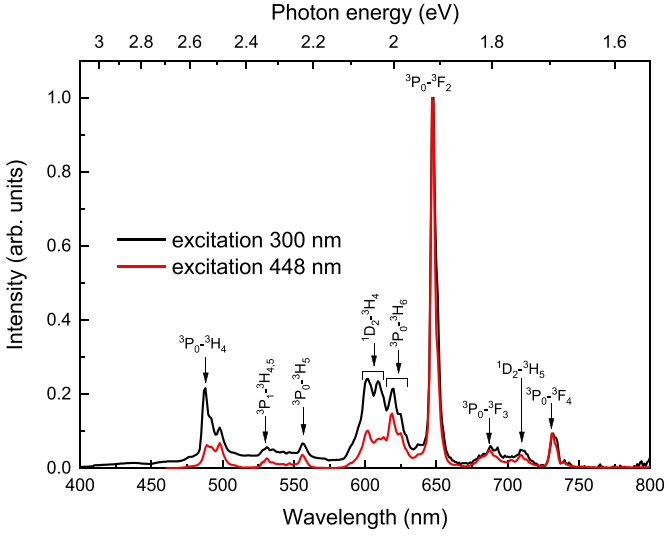

Fig. 8. Luminescence emission spectra at room temperature of $SrMoO_4$ crystals doped with Pr^{3+} (luminescence excitation 300 nm, which corresponds to LMCT excitation band, and 448 nm, which corresponds to Pr^{3+} transition $^3H_4$–$^3P_2$). Luminescence spectra are normalized at maximum intensity.

intensity of the LMCT band is comparably lower in comparison with the rare-earth ion signals than it is for Eu-doped single crystals.

3.3. Temperature dependency of luminescence

Thermal quenching of the LMCT band in the luminescence spectra has been observed in pure and doped $SrMoO_4$. The temperature dependency of the emission excited in the LMCT band in the UV region is shown in Figs. 10–12. The intensity of the luminescence emission decreases significantly already after 20 K with complete quenching at room temperature. The intensity of the charge transfer band in Pr- and Eu-doped single crystals is high enough to dominate the luminescence spectra at low temperatures, making it impossible to elucidate whether the intensity of 4f-4f transitions of rare-earth ions is temperature-dependent in $SrMoO_4$ single crystals. However, it is clear from Fig. 12

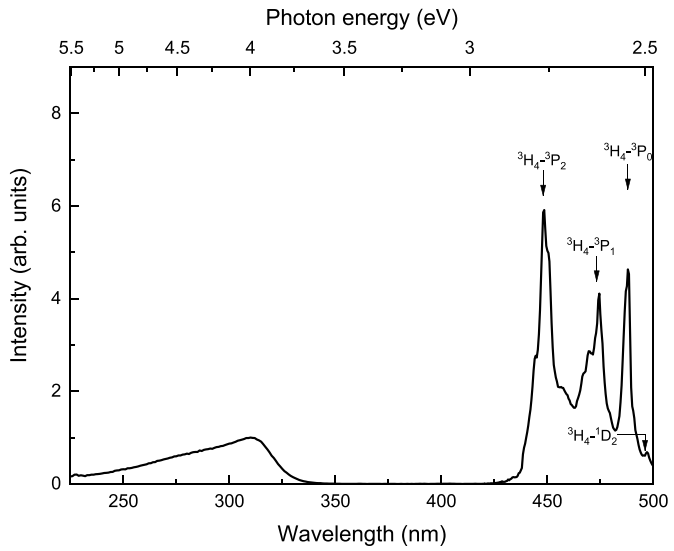

Fig. 9. Luminescence excitation spectra at room temperature of $SrMoO_4$ crystals doped with Pr^{3+} (luminescence emission 300 nm). Luminescence spectra are normalized at maximum intensity.

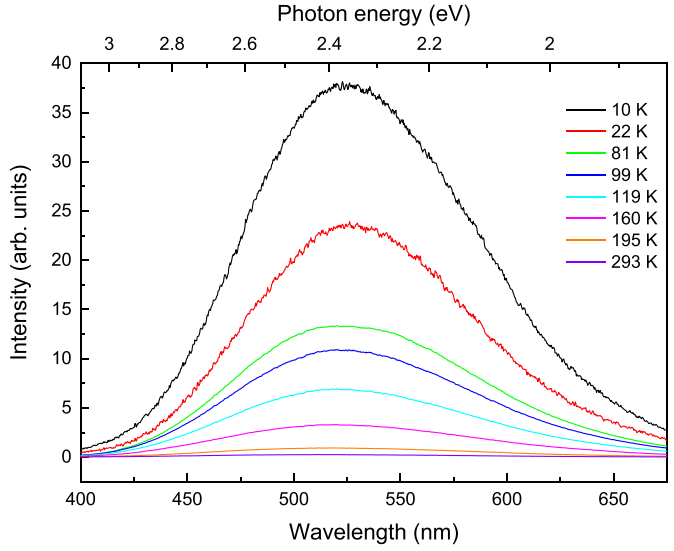

Fig. 10. The temperature dependency of the luminescence spectra of undoped $SrMoO_4$ single crystal (luminescence excitation 300 nm).

that the intensity ratio of LMCT emission and Eu^{3+} signals is directly dependent from the concentration of Eu^{3+} in the single crystals (see Fig. 12 and Figs. S2 and S3 in supplementary).

The thermal quenching of LMCT emission band can be explained using the approximation of Mott-Seitz formula [22]. The Mott-Seitz mechanism explains the thermal quenching by the competition of radiative and non-radiative recombination. According to this model, the light yield of luminescence emission is:

$$LY = \frac{1}{1 + C \cdot e^{-\frac{E_a}{k_B T}}},$$

where LY – luminescence light yield, E_a – activation energy of thermal quenching (eV), k_B – Boltzmann constant ($8.62 \cdot 10^{-5}$ eV K^{-1}), T – temperature (K), C – constant.

By plotting the luminescence intensity logarithmic function lnI versus reverse temperature 1/T thermal quenching activation energy can be found from the slope of approximated function (example of a

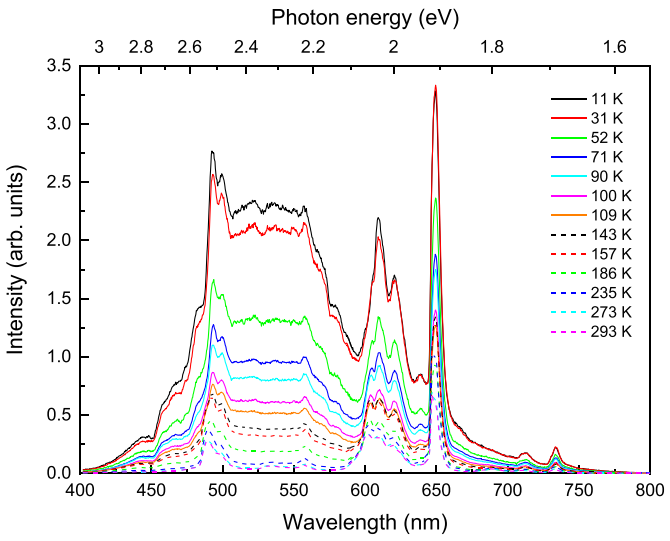

Fig. 11. The temperature dependency of $SrMoO_4$:Pr single crystal (luminescence excitation 275 nm).

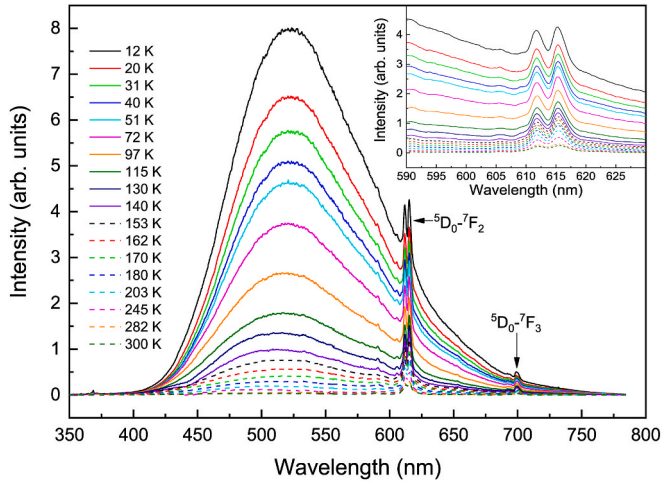

Fig. 12. The temperature dependency of $SrMoO_4$:Eu (0.1 wt% $EuNbO_4$) single crystal (luminescence excitation 275 nm).

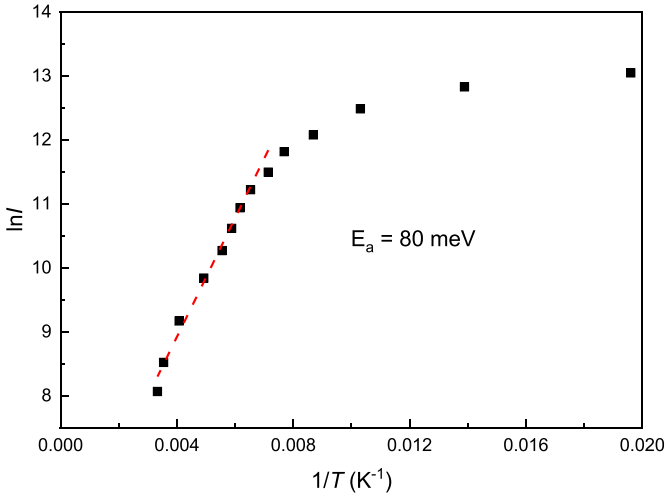

Fig. 13. Temperature dependency of luminescence of LMCT band in Eu-doped $SrMoO_4$ (0.1 wt% $EuNbO_4$).

graph in Fig. 13). Activation energies of pure and doped $SrMoO_4$ single crystals are compared in Table 1 and their dependency from dopant concentration is compared in Fig. 14. It has been established that an increase of rare-earth dopant concentration decreases necessary energy for luminescence thermal quenching.

We propose that the decrease of activation energy values due to an increased Eu^{3+} content is happening similarly to the well-known mechanism in semiconductors. The increase in the concentration of impurities in semiconductors is followed by the lowering of the conduction band edge, the shift of the ground-state energy level of the donor due to conduction electron screening as well as the broadening of the impurity level [23–25]. In our opinion, this mechanism may also be applied to $SrMoO_4$ single crystals.

The temperature dependency of luminescence decay kinetics has also been studied. Fig. 15 shows the decay kinetics of undoped $SrMoO_4$ under tunable laser excitations. The luminescence excitation of 250 nm corresponds to the band-to-band transition. The luminescence decay has a form of the double exponential function with a fast component corresponding to the influence of the laser as we assume. The slower component of the luminescence decay is highly dependent from the temperature of the single crystal, with luminescence decay rapidly quickening at temperatures higher than 100 K.

Similar results have been obtained with the doped single crystals. Decay times of intrinsic emission at different temperatures of pure and doped $SrMoO_4$ have been obtained and compared in Fig. 16. No dependency has been observed between luminescence decay times of intrinsic emission of doped and undoped $SrMoO_4$ single crystals and the concentration of the dopant ions. We suggest that an identical crystalline defect is present in all the studied $SrMoO_4$ single crystals. This way recombination through the defect would occur with the same decay time independent of rare-earth dopant nature and concentration.

4. Conclusions

The pure and doped with Pr^{3+} (1.0 wt% $PrNbO_4$) and different concentrations of Eu^{3+} (0.1 wt% $EuNbO_4$, 0.22 wt% $EuNbO_4$ and 0.5 wt % $EuNbO_4$) $SrMoO_4$ single crystals were obtained by means of Czochralski method. The broad intensive absorption band at 3 eV in Eu-doped $SrMoO_4$ has been detected and explained by Eu^{2+} center. Luminescence properties of pure and rare-earth doped $SrMoO_4$ have been studied. Temperature dependency of the intrinsic emission of both doped and undoped $SrMoO_4$ has been measured, as well as activation energies of thermal quenching of luminescence have been calculated. Temperature dependencies of decay times of intrinsic luminescence both in undoped and doped $SrMoO_4$ single crystals have been measured. The independence of the temperature behavior of decay time of intrinsic luminescence from rare-earth dopants is explained by relaxation of excitations through defect states which are similar in all $SrMoO_4$ single crystals studied.

CRediT authorship contribution statement

Viktorija Pankratova: Experiments, Writing, Funding Acquisition, Investigation; **Elizaveta E. Dunaeva, Irina S. Voronina:** Synthesis and Crystal Growth; **Anna P. Kozlova:** Experiments; **Roman P. Shendrik:**

Table 1
Activation energies of luminescence thermal quenching in $SrMoO_4$ single crystals.

Dopant	E_a (meV)
–	70
0.1 wt% $EuNbO_4$	80
0.22 wt% $EuNbO_4$	73
0.5 wt% $EuNbO_4$	69
1 wt% $PrNbO_4$	63

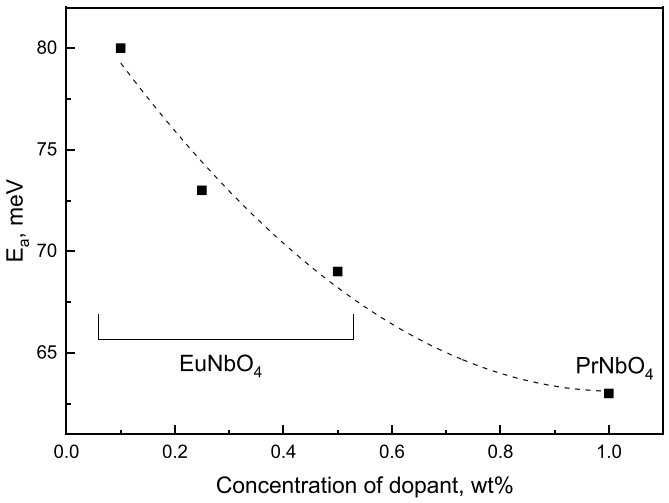

Fig. 14. Dependency of activation energies of thermal quenching from dopant concentration in $SrMoO_4$ single crystals (dashed line is shown for better visualization).

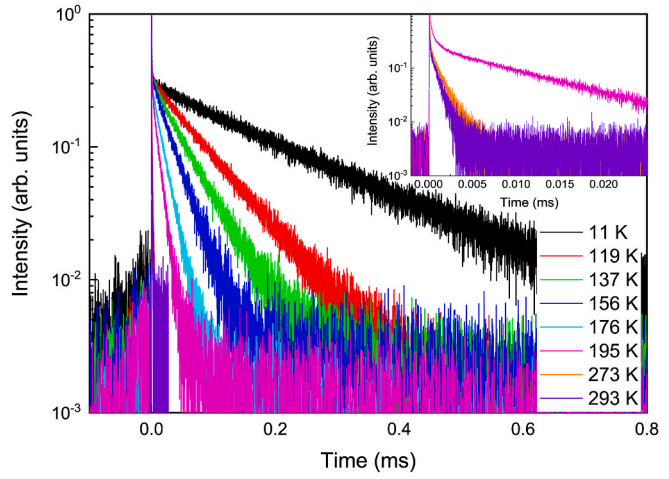

Fig. 15. Temperature dependency of decay kinetics of pure $SrMoO_4$ single crystal (excitation 250 nm, emission 470 nm).

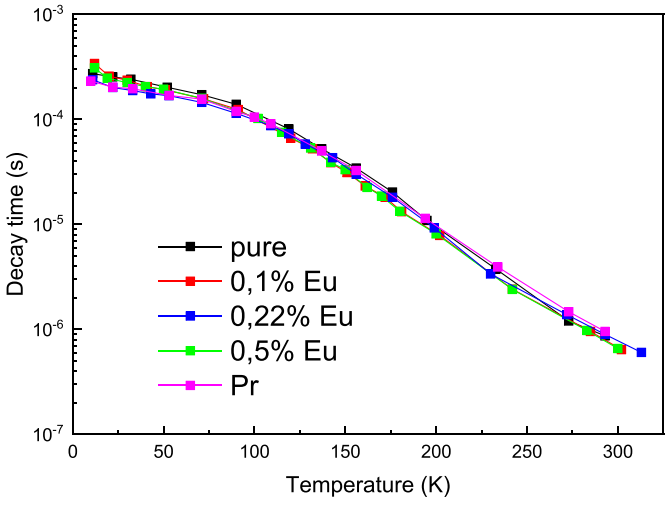

Fig. 16. Temperature dependency of decay times in pure and rare-earth doped $SrMoO_4$ single crystals.

Experiments, Writing; **Vladimir Pankratov:** Conceptualization, Writing.

Declaration of competing interest

The authors declare that they have no known competing financial interests or personal relationships that could have appeared to influence the work reported in this paper.

Acknowledgments

The work of V. Pankratova was supported by the financial support of Scientific Research Project for Students and Young Researchers (SJZ/2020/05) realized at Institute of Solid State Physics, University of Latvia. The Institute of Solid State Physics, University of Latvia as the Center of Excellence has received funding from the European Union's Horizon 2020 Framework Programme H2020-WIDESPREAD-01-2016-2017-TeamingPhase2 under grant agreement No. 739508, project CAMART^2.

Appendix A. Supplementary data

Supplementary data to this article can be found online at https://doi.org/10.1016/j.omx.2022.100169.

References

[1] R.L. Tranquilin, L.X. Lovisa, C.R.R. Almeida, C.A. Paskocimas, M.S. Li, M. C. Oliveira, L. Gracia, J. Andres, E. Longo, F.V. Motta, M.R.D. Bomio, Understanding the white-emitting $CaMoO_4$ Co-doped Eu^{3+}, Tb^{3+}, and Tm^{3+} phosphor through experiment and computation, J. Phys. Chem. C 123 (2019) 18536–18550, https://doi.org/10.1021/acs.jpcc.9b04123.

[2] H. Wu, Y. Hu, W. Zhang, F. Kang, N. Li, G. Ju, Sol-gel synthesis of Eu^{3+} incorporated $CaMoO_4$: the enhanced luminescence performance, J. Sol. Gel Sci. Technol. 62 (2012) 227–233, https://doi.org/10.1007/s10971-012-2716-8.

[3] L. Li, P. Yang, W. Xia, Y. Wang, F. Ling, Z. Cao, S. Jiang, G. Xiang, X. Zhou, Y. Wang, Luminescence and optical thermometry strategy based on emission and excitation spectra of Pr^{3+} doped $SrMoO_4$ phosphors, Ceram. Int. 47 (2021) 769–775, https://doi.org/10.1016/j.ceramint.2020.08.187.

[4] S.K. Ray, J. Hur, Surface modifications, perspectives, and challenges of scheelite metal molybdate photocatalysts for removal of organic pollutants in wastewater, Ceram. Int. 46 (2020) 20608–20622, https://doi.org/10.1016/j.ceramint.2020.05.245.

[5] A. Kuzmanoski, V. Pankratov, C. Feldmann, Microwave-assisted ionic-liquid-based synthesis of highly crystalline $CaMoO_4$: RE^{3+} (RE = Tb, Sm, Eu) and $Y_2Mo_4O_{15}$:Eu^{3+} nanoparticles, Solid State Sci. 41 (2015) 56–62, https://doi.org/10.1016/j.solidstatesciences.2015.02.005.

[6] F. Baur, T. Jüstel, Eu^{3+} activated molybdates – structure property relations, Opt. Mater. X. 1 (2019), https://doi.org/10.1016/j.omx.2019.100015.

[7] S. Shionoya, W.M. Yen, H. Yamamoto, Phosphor Handbook, second ed., CRC Press, Boca Raton, 2006.

[8] C. Gan, X. Xu, J. Yang, Z. Peng, Preparation and luminescence properties of $SrMoO_4$ doped with Pr^{3+}, in: Key Eng. Mater., Trans Tech Publications Ltd, 2014, pp. 253–256. https://doi.org/10.4028/www.scientific.net/KEM.633.253.

[9] E.E. Dunaeva, L.I. Ivleva, M.E. Doroshenko, P.G. Zverev, V.V. Osiko, $SrMoO_4$:Pr^{3+} single crystals: growth and properties, Dokl. Phys. 60 (2015) 122–126, https://doi.org/10.1134/S102833581503009X.

[10] J. Shu, Z. Jia, E. Damiano, H. Wang, Y. Yin, N. Lin, X. Zhao, X. Xu, M. Tonelli, X. Tao, Charge compensations of Eu^{2+} and O_i^{2-} co-exist in Eu^{3+}:$CaMoO_4$ single-crystal fibers grown by the micro-pulling-down method, CrystEngComm 20 (2018) 6741–6751, https://doi.org/10.1039/C8CE01160E.

[11] A.D. Gorlov, ^{151,153}Eu electron paramagnetic resonance in $SrMoO_4$ and determination of signs of spin Hamiltonian parameters at different temperatures, Phys. Solid State 56 (2014) 2185–2190, https://doi.org/10.1134/S1063783414110080.

[12] A. Yoshikawa, V. Chani, M. Nikl, Czochralski growth and properties of scintillating crystals, Acta Phys. Pol., A 124 (2013) 250–264, https://doi.org/10.12693/APhysPolA.124.250.

[13] F. Zhu, Z. Xiao, L. Yan, F. Zhang, A. Huang, The influence on intrinsic light emission of calcium tungstate and molybdate powders by multivalence Pr codoping, Appl. Phys. Mater. Sci. Process 101 (2010) 689–693, https://doi.org/10.1007/s00339-010-5950-3.

[14] N. Niu, P. Yang, W. Wang, F. He, S. Gai, D. Wang, J. Lin, Solvothermal synthesis of $SrMoO_4$:Ln (Ln = Eu^{3+}, Tb^{3+}, Dy^{3+}) nanoparticles and its photoluminescence properties at room temperature, Mater. Res. Bull. 46 (2011) 333–339, https://doi.org/10.1016/j.materresbull.2010.12.016.

[15] M. Guzik, E. Tomaszewicz, Y. Guyot, J. Legendziewicz, G. Boulon, Eu^{3+} luminescence from different sites in a scheelite-type cadmium molybdate red

phosphor with vacancies, J. Mater. Chem. C 3 (2015) 8582–8594, https://doi.org/10.1039/c5tc01109d.
[16] W. Feng, H. Lin, H. Liu, Photoluminescence and crystal-field analysis of Pr^{3+}-doped $SrMoO_4$ phosphors, Z. Naturforsch. 70 (2019) 11–16, https://doi.org/10.1515/zna-2014-0184.
[17] S.K. Gupta, M. Sahu, P.S. Ghosh, D. Tyagi, M.K. Saxena, R.M. Kadam, Energy transfer dynamics and luminescence properties of Eu^{3+} in $CaMoO_4$ and $SrMoO_4$, Dalton Trans. 44 (2015) 18957–18969, https://doi.org/10.1039/c5dt03280f.
[18] J.B. Gruber, U.V. Valiev, G.W. Burdick, S.A. Rakhimov, M. Pokhrel, D.K. Sardar, Spectra, energy levels, and symmetry assignments for Stark components of $Eu^{3+}(4f^6)$ in gadolinium gallium garnet ($Gd_3Ga_5O_{12}$), J. Lumin. 131 (2011) 1945–1952, https://doi.org/10.1016/J.JLUMIN.2011.03.057.
[19] J.C. Peixoto, A. Dias, F.M. Matinaga, K.P.F. Siqueira, Luminescence properties of $PrNbO_4$ and $EuNbO_4$ orthoniobates and investigation of their structural phase transition by high-temperature Raman spectroscopy, J. Lumin. 238 (2021), 118284, https://doi.org/10.1016/j.jlumin.2021.118284.
[20] K. Thomas, D. Alexander, S. Sisira, S. Gopi, P.R. Biju, N.V. Unnikrishnan, C. Joseph, Energy transfer driven tunable emission of Tb/Eu co-doped lanthanum molybdate nanophosphors, Opt. Mater. 80 (2018) 37–46, https://doi.org/10.1016/j.optmat.2018.04.010.
[21] X. Liu, L. Li, H.M. Noh, B.K. Moon, B.C. Choi, J.H. Jeong, Chemical bond properties and charge transfer bands of O^{2-}-Eu^{3+}, O^{2-}-Mo^{6+} and O^{2-}-W^{6+} in Eu^{3+}-doped garnet hosts $Ln_3M_5O_{12}$ and ABO_4 molybdate and tungstate phosphors, Dalton Trans. 43 (2014) 8814–8825, https://doi.org/10.1039/C4DT00674G.
[22] N.F. Mott, R.W. Gurney, Electronic Processes in Ionic Crystals, second ed., Clarendon Press, Oxford, 1948.
[23] G.L. Pearson, J. Bardeen, Electrical properties of pure silicon and silicon alloys containing boron and phosphorus, Phys. Rev. 75 (1949) 865, https://doi.org/10.1103/PhysRev.75.865.
[24] G.F. Neumark, Concentration and temperature dependence of impurity-to-band activation energies, Phys. Rev. B 5 (1972) 408–417, https://doi.org/10.1103/PhysRevB.5.408.
[25] T.F. Lee, T.C. McGill, Variation of impurity−to−band activation energies with impurity density, J. Appl. Phys. 46 (1975) 373, https://doi.org/10.1063/1.321346.